HHS Public Access

Author manuscript

Carbon N Y. Author manuscript; available in PMC 2019 April 19.

Published in final edited form as:

Carbon N Y. 2013 August ; 60: 67–75. doi:10.1016/j.carbon.2013.03.057.

Disruption of Model Cell Membranes by Carbon Nanotubes

Charlie Corredor[1], **Wen-Che Hou**[4], **Steven A. Klein**[3], **Babak Y. Moghadam**[2], **Michael Goryll**[5], **Kyle Doudrick**[4], **Paul Westerhoff**[4], and **Jonathan D. Posner**[1,2,*]

[1]Chemical Engineering, University of Washington, Seattle, WA 98115

[2]Mechanical Engineering, University of Washington, Seattle, WA 98115

[3]Mechanical Engineering, Arizona State University, Tempe, Arizona 85287-6106

[4]Environmental Engineering, Arizona State University, Tempe, Arizona 85287-6106

[5]Electrical Engineering, Arizona State University, Tempe, Arizona 85287-6106

Abstract

Carbon nanotubes (CNTs) have one of the highest production volumes among carbonaceous engineered nanoparticles (ENPs) worldwide and are have potential uses in applications including biomedicine, nanocomposites, and energy conversion. However, CNTs possible widespread usage and associated likelihood for biological exposures have driven concerns regarding their nanotoxicity and ecological impact. In this work, we probe the responses of planar suspended lipid bilayer membranes, used as model cell membranes, to functionalized multi-walled carbon nanotubes (MWCNT), CdSe/ZnS quantum dots, and a control organic compound, melittin, using an electrophysiological measurement platform. The electrophysiological measurements show that MWCNTs in a concentration range of 1.6 to 12 ppm disrupt lipid membranes by inducing significant transmembrane current fluxes, which suggest that MWCNTs insert and traverse the lipid bilayer membrane, forming transmembrane carbon nanotubes channels that allow the transport of ions. This paper demonstrates a direct measurement of ion migration across lipid bilayers induced by CNTs. Electrophysiological measurements can provide unique insights into the lipid bilayer–ENPs interactions and have the potential to serve as a preliminary screening tool for nanotoxicity.

1. INTRODUCTION

There is a growing interest in understanding the toxic potential and environmental impact of engineered nanoparticles (ENPs).[1,2] Due to their unique properties, ENPs have found a wide range of applications in over 1,300 commercial products such as drug delivery carriers,

*Corresponding Author. Phone: +1 (206) 543-9834 (J. D. P.). Fax: +1 (206) 685-8047. jposner@uw.edu (J. D. P.).

SUPPORTING INFORMATION

Additional information on MWCNTs TEM imaging, ENPs zeta potentials, and representatives of ENPs current traces at multiple mass concentrations can be found at the supporting information of this paper.

cosmetics, antibiotics, bioimaging, nanoelectronics, etc.[3] ENPs are anticipated to ultimately come into contact with biological systems, considering that some ENP-containing products are designed for direct human contact (e.g., food, cosmetics, drug delivery) and that they will be released into the environment at some point in their life cycle such as during manufacturing, usage, or disposal. However, understanding the dynamic processes at the interface between biological membranes and ENPs is still in its nascent stages.[4] Probing the interactions of ENPs at the biological interface may aid in the understanding of potential toxicity, design of safe nanoproducts, and advancement of nanomedicine.[4,5]

Lipid bilayers, which mimic the natural fluidity and permeability of cellular membranes, constitute a continuous barrier between cells and their environment.[6,7] The contact of engineered nanoparticles with lipid bilayers is important because it is one of the first steps towards subsequent biological effects. Our review study and previous work have attempted to elucidate ENPs' effect on lipid membrane integrity and their relevancy to cell-ENP interaction.[8] Leroueil et al. used atomic force microscopy on a supported lipid bilayer to detect pore formation and thinning of lipid membranes by the exposure of cationic engineered nanoparticles.[9] Each cationic particle presented in their work, despite the shape, chemical composition, size, deformability, or charge density, disrupted the lipid membranes integrity by forming holes in the membrane.[9] Similarly, Goodman et al. showed that positively charged gold nanoparticles (2 nm) increase the permeability of cell membranes and lipid vesicles (i.e., liposomes) more than anionic gold nanoparticles.[10] In a similar fashion, we have detected leakage from 100 nm unilamellar liposomes, via fluorescence spectroscopy, upon their exposure to 10 nm metal and metal oxide ENPs with different surface functionalities, at concentrations down to 30 ppb.[11] We found that liposome leakage increases with the ENPs' number density. Our data shows that leakage is mediated by electrostatic interactions that are primarily governed by the ENP surface functional groups and is not dependent on the particle core composition. We found that, on average, only one particle per liposome is required to disrupt membranes. We examined the lipid bilayer-water distribution of functionalized gold, C_{60}, and fullerene ENPs with the aim of developing quantitative methods that can be used to predict the bioaccumulation, ecotoxicology (e.g. aquatic environments), transport, and fate of these materials.[12–14] This work showed that the adsorption of ENP to bilayers is also largely governed by electrostatic forces.

Carbon nanotubes (CNTs) production and usage is rapidly growing.[15] There is concern over carbonaceous nanomaterial's toxicity and fate in the environment due to their use in biomedicine, nanocomposites, and energy conversion.[16] Previous studies have shown that CNTs can exert toxic effects on cells such as oxidative stress, inflammation, inhibition of cell growth and activity, etc.[7,17–20] Recent works by Semberova et al. and De Paoli et al. have shown that CNTs induced aggregation of blood platelets as well as provoked an influx of extracellular ions through cell membranes.[21,22] These studies demonstrated the ability of CNTs to penetrate plasma membranes without noticeable membrane damage. Similarly, Kang et al. showed a direct correlation between physicochemical modifications of CNTs and cytotoxic effect that this carbonaceous nanomaterial has in *Escherichia coli*. [23] This work showed a higher toxic effect in bacterial systems when the nanotubes are uncapped, debundled, short in length, and well dispersed in media. Collectively, these studies suggest

that CNTs compromise cellular membranes and induce leakage of intracellular contents or influx of extracellular materials. Molecular simulation studies also indicate that CNTs can penetrate lipid bilayers[24] and transport water, biomolecules as well as ions by creating artificial biomembrane channels.[25–28] However, there is no experimental evidence that CNTs can disrupt lipid bilayers and modulate a bilayers natural resistance to the flux of ions and molecules.

Electrophysiological measurements, such as patch clamp techniques, are capable of quantifying small electrical currents passing through cellular membranes as well as suspended planar lipid bilayers. The great sensitivity of electrophysiological measurements in detecting current fluctuations on the order of picoamperes (pA) across the perturbed membranes have made these techniques widely employed to monitor the formation of ion channels,[29,30] to measure the fusion of lipid membranes via single-channel recordings,[31] and to study electroporation.[32] These techniques have also been used to probe the interaction of ENP with cells and lipid bilayers. Chen et al. reported that a range of cationic polymer nanoparticles induced current fluxes across living human cell membranes and estimated the formation of nanoscale hole defects ranging from 3 to 20 nm.[33] Ramachandran et al. and our group have shown that water-soluble CdSe/ZnS quantum dots (QD) induce current flux across planar lipid bilayer membranes (pBLMs), which are protein free phospholipid bilayers suspended across a ~150 μm diameter aperture.[34,35] We correlated the current fluctuations induced by QDs adsorption on pBLMs with fluorescent microscopy.[35] Our measurements showed that electrical fluctuations occur when QDs adsorb and aggregate on fluid lipid bilayers. This work suggests that QD aggregates form nanoscale pore defects (~2 nm), which allow the passage of ions. However, there was not experimental evidence on how ENPs' concentration affects lipid membrane disruption and quantification methods that describe this interaction. More recently, de Planque et al. used electrophysiological measurements to evaluate the ENP disruption of lipid membranes on suspended planar lipid bilayers that are formed by bringing two monolayer lipid microdroplets into contact within a microfluidic channel.[36] All these prior studies collectively demonstrate that there are significant ENP-lipid bilayer interactions (e.g. adsorption, disruption, etc.) and suggest that these interactions may be indicative of cellular responses to ENPs and toxicity effects.

In this paper, we report on the interaction of functionalized multi-walled carbon nanotubes (MWCNTs) with 1,2-dioleyl-sn-3-phosphatidylcholine (DOPC) lipid bilayers as model cell membranes using electrophysiological measurements on pBLM. We focus on MWCNTs, because they are carbonaceous ENPs with the highest volume manufacturing worldwide with an estimate production rate of 3400 ton/yr.[15] In this work, we use carboxyl functionalized MWCNTs, which have been characterized in a wide range of toxicity assays as part of the NIEHS NANO-GO consortium.[37,38] Here, we compare the lipid bilayer disruption behavior of MWCNTs with that of QDs, and melittin, a well-known pore-forming peptide.[39–41] We quantify the current flux events resulting from lipid bilayer-ENP interactions by calculating the fractional event interaction (FEI) and average conductance as a function of multiple ENPs' concentrations. The results show that the MWCNT disrupt the bilayer in a different mechanism than melittin and QDs, which require aggregate complexes to cause leakage. Our data suggest that MWCNTs insert and traverse the lipid bilayer

membrane, forming transmembrane carbon nanotubes channels that transport ions. Current fluxes patterns, FEI, and average conductance calculations of ENPs are used to shed light on the possible interaction mechanism of lipid membrane disruptions.

2. EXPERIMENTAL SECTION

2.1 Materials and Methods

We examined the interactions of ENPs with suspended planar lipid bilayers using electrophysiological measurements. We used functionalized carboxyl MWCNTs obtained as a consortium material from NIEHS NANO-GO where their fabrication and characterization have been documented in a previous reports.[37,38] MWCNTs have a reported outer diameter of 20–25 nm, an inner diameter of 5–10 nm, and a length of 10–30 μm, as confirmed by TEM, shown in Figure S1. The MWCNTs have a reported purity greater than 99% by weight as carbon nanotubes with no metal catalyst impurity measured by thermogravimetric analyses.[37] The carboxyl functionalized MWCNT stock solution was prepared by dispersing dry powder (10 mg/10 mL) in ultrapure water (18.3 MΩ-cm, Nanopure®) followed by mild sonication for 1 h (40 Hz, 2510DTH Branson, Ultrasonic Corp., Danbury, CT). We compared the MWCNT results with carboxyl CdSe/ZnS QDs (Q21341MP - Invitrogen, Eugene, OR) and melittin (CAS: 20449-79-0 Sigma Aldrich St. Louis, MO), a peptide well known to disrupt lipid membranes. We dissolved 5 mg/mL of the dry melittin powder in 20 mM N-(2-hydroxyethyl)piperazine-N′-(2-ethanesulfonic acid) (HEPES) buffer (CAS: 7365-45-9 Sigma Aldrich St. Louis, MO) at pH = 7.4 and kept frozen at −20°C. The melittin sample was thawed at 23°C prior to use.

Our suspended lipid bilayers were constituted by 1,2-dioleyl-sn-3-phosphatidylcholine (DOPC) lipids (CAS: 4235-95-4 Avanti Polar Lipids, Alabaster, AL). 20 mM HEPES and 20 mM KCl at pH = 7.4 was used in all experiments, prepared using purified water (Milli-Q Advantage A10 ® system, Millipore Corp., Billerica, MA). We chose this electrolyte to keep the electrophysiological measurement signal to noise ratio as large as possible (i.e., higher conductivity results in larger signal to noise) without sacrificing particle stability (i.e., aggregation due to reduction in electric double layer thickness or surface charge). We did not use any surfactants or dispersion stabilizing chemicals so as to avoid any other perturbation of the suspended lipid membrane.

We measured the hydrodynamic size and zeta potential of the particles and lipids membranes using dynamic light scattering (DLS) (NICOMP 380 ZLS, Particle Sizing Systems, Santa Barbara, CA) over a 60 min time period, during which typical interaction experiments were performed. The relationship between the size of particles and their Brownian motion is described by the Stokes-Einstein equation.[42] The zeta potentials of particles influence their electrophoretic mobility, as describe by the Henry equation and the Smoluchowski approximation.[43] DOPC lipids zeta potential were measured using liposomes that were prepared using the extrusion method.[44] Briefly, dry DOPC lipid powder was dissolved in chloroform and then dried with N_2. The resulting lipid film was hydrated with the same buffer electrolyte solution (20 mM HEPES with 20 mM KCl) under vortex mixing to form multilamellar liposome suspensions. The suspensions were passed through polycarbonate membrane filters with a pore size of 100 nm using a commercial

extruder (LIPEX, Northern Lipids Inc., BC, Canada) 11 times to obtain ~100 nm unilamellar liposomes.

2.2 Electrophysiological Measurement Platform

We examined the interactions of ENPs with suspended lipid bilayer membranes using electrophysiological measurements by continuously monitoring the current across the suspended pBLM (Figure 1). 3 ml polystyrene reservoirs (i.e., cis and trans) (Warner Instruments LLC., Hamden, CT) are separated by a 150 μm diameter aperture over which the lipid bilayer is suspended. The reservoir chamber is mounted in a Faraday cage on a vibration isolation table to achieve optimal shielding from spurious electromagnetic radiation and reduction of mechanical noise. A low-noise extracellular patch clamp amplifier (EPC8, HEKA Instruments Inc., Bellmore, NY) with Ag/AgCl electrodes immersed into each reservoir measured the current that migrates across the bilayer. The current passing through the bilayer is amplified, filtered with a low-pass, 8-pole Bessel filter at 1 kHz, sampled at 10 kHz (National Instrument, PCIe-6251 DAQ board), recorded using a custom LabView script, and processed with an in-house Matlab code. A positive ion migration flux from the cis to the trans compartment is measured as positive current. All experiments presented in this paper were conducted at ~20°C.

The suspended lipid bilayer was painted across the 150 μm aperture using the conventional Montal-Mueller technique.[45] First, a DOPC (0.4 mL at 10 mg/mL) in chloroform solution was placed in a test tube and dried by a gentle stream of pure N_2 gas and left in a desiccator overnight. The dry lipid film was reconstituted in 1 mL of decane. The DOPC lipid solution was freshly prepared immediately prior to every use to minimize potential variability in the lipid membrane permeability. Next, we primed the 150 μm aperture with a small quantity of lipids prior to adding electrolyte. Then 3 mL HEPES-KCl buffer electrolyte was added to each reservoir in an effort to minimize the differential hydrostatic pressure across the reservoirs. We painted the membrane by immersing a pipette in the DOPC lipid solution and gently spreading it on the working aperture using the Montal-Mueller technique.[45] A true bilayer exhibits a high resistance of ~10 GΩ and the ability to be ruptured with a voltage pulse.[34,35,46] We examined the existence of proper pBLM by applying a 500 mV voltage pulse to rupture the bilayer. This experimental step is repeated three times to confirm of a proper bilayer membrane formation before initiating experiments by adding nanoparticles to the cis reservoir. For the case of MWCNTs experiments, we mixed the particle suspension in situ with a stirring bar for 5 s prior to recording the current flux, which is a standard practice in pBLM measurements when studying ion channels.[40,47,48]

We performed experiments to ensure that adsorption of the particles to the bilayer and subsequent disruption was not induced by the applied electric field. In some experiments we reversed the field and still measured similar disruptions. We conducted experiments where the applied voltage was set to zero for several minutes to allow the particles to interact. When turning the voltage back up to 100 mV we observed electrical currents that were consistent with the time that had transpired with the amplifier off. These experiments provide confidence that the electric field generated by the amplifier does not significantly contribute the observed ENP interaction with the bilayer.

3. RESULTS AND DISCUSSION

3.1. Lipid bilayer and ENPs Characterization

We measured the zeta potential and particle sizes every 15 minutes for a total time of 60 min period. Over this time, the measured size and charge remained relatively constant, suggesting that the particles do not aggregate in HEPES-KCl buffer (pH 7.4, 20 mM). Hydrodynamic sizes and zeta potentials of particles are reported herein as means of triplicate measurements. The MWCNTs had an average hydrodynamic diameter of 112.0 ± 0.46 nm (one standard deviation) and an average zeta potential of −16.0 ± 0.7 mV. Although the use of DLS is not appropriate for non-spherical particles or for long-aspect ratio materials, we obtained semi-quantative data to show the lack of aggregation in our buffer solution. This measured size correlates with the size revealed by TEM micrographs of MWCNTs (Figure S1). The QDs had an average hydrodynamic diameter of 12.7 ± 0.79 nm and an average zeta potential of −9.8 ± 1.1 mV. The melittin and DOPC lipids revealed an average zeta potential of 13.4 ± 1.1 and −12.1 ± 1.5 mV, respectively (Table S1).

3.2 Lipid Bilayer and ENPs Interactions

A set of representative nanoparticle and suspended lipid bilayer interactions are shown on Figure 2. In the absence of nanoparticles (Figure 2A), the current passing through the lipid bilayer was very low at ~8 pA at an applied voltage of 100 mV and remained steady for a period of ~600 s. The lipid membrane created a good ion flux seal with a resistance of ~8 GΩ, as measured by applying a ramp voltage and determining the slope of the resulting current-voltage curve. The low bilayer current flux is consistent with the fact that bilayers serve as an effective barrier to the flux of ions as shown in prior studies.[34–36] The low current flux and the ability of facile disruption after the application of a 500 mV voltage pulse confirms the formation of a suspended lipid bilayer. Our bilayers were typically stable for ~20 h. To the right of Figure 2A, we report normalized histograms of current flux events. The normalized histograms are discrete estimates of probability density functions defined as,

$$H_j = \frac{N_j}{\sum_j N_j} \quad 1$$

where N_j is number of events in bin j at a given current. Figure 2A displays a single peak spanning from 4.5 to 10.5 pA and a mean of 8 pA, which represents the baseline current due to the intrinsic ion permeability of the lipid bilayer and instrument noise under the applied electric field.

Figure 2B shows the current flux across the suspended lipid bilayer induced by 6 ppm melittin, our reference organic compound that is well know to generate pores in lipid membranes. After 10s of melittin exposure, we observe an initial sharp current burst (~50 pA) that lasts for 90 ms. Next, a current step of ~80 pA occurred at 83.5 s that lasts for ~300 ms. The current bursts became more intense and frequent, eventually resulting in total membrane failure after 600 s. This disruption of the membrane was consistently observed at all studied concentrations, shown in Figure S2 A and B. The histogram shows a distinctive

current peak at 147 pA or 1.47 nS, corresponding to the multiple bursts shown in inset on Figure 2B. The spontaneous formation and temporal instability of the current signatures is thought to influenced by the peptide's Brownian motion. These results are consistent with previous studies that also reported burst-like current traces due to defined nanopores formed from four or more melittin molecules.[40,47] Melittin incorporates into lipid membranes and induces sporadic disruption and current signals (i.e., pore formation) due to Brownian rearrangement and conformational changes of the peptides in the membrane association.

Upon the addition of carboxyl QDs at 6 ppm we observe similar current-time traces to melittin, as shown in Figure 2C. Initially, the current flux remained steady at the baseline level, similar to what is observed in the control and melittin experiments, suggesting that there is no interaction of the QDs with the bilayer. A first set of current bursts is later observed at 500 s with an event time duration of ~200 ms and maximum current amplitude of 40 pA. The current bursts in the presence of QDs occur intermittently with peak currents varying from 10 to 105 pA. 210 s after the first interaction event, we observe larger and more frequent current fluctuations at amplitudes between 15 to 105 pA with an average current of 60 pA. The QDs do not cause a complete lipid bilayer failure at this concentration or at 60 ppm (see Figure S2 C). The histogram of Figure 2C presents a broadened primary peak at 7 pA and a second broad peak centered at 60 pA. The primary peak at 7 pA, which represents the baseline signal, has an extended tail into higher currents because of low magnitude current spikes induced by QDs. The secondary peak in the histogram at 60 pA or 0.6 nS represents an increase in the membranes permeability due to QDs. These current fluctuations has been attributed to the oligomeric aggregation of QDs onto the bilayer that creates nanopore defects on the lipid bilayer, through which ion transport occurs.[34,35] We previously showed that QDs aggregate on membranes and diffuse freely allowing the passage of ions.[35] This current signature of QDs is similar to melittin, which suggests that they too require an aggregate of particles to induce ion leakage. Spherical, carboxyl polymeric nanoparticles have also shown to create pores on supported lipid bilayers.[49] The sporadic current bursts in the data suggest that the defects induced by QDs open and close intermittently, similar to melittin.

Figure 2D reports the current flux across the suspended lipid bilayer induced by MWCNTs at 6 ppm. In contrast to melittin and QDs, MWCNTs interacted with the suspended lipid membrane more rapidly (typically within ~5 s) and in a stepwise manner. MWCNTs induced a rapid increase in trans-membrane current of ~50 pA followed by a short plateau lasting for 4 s. We then observe a drastic escalation of current to 950 pA during an 11 s time lapse. The current then remained constant for 20 s and then rapidly increased to 1200 pA. The current flux increased in steps, with each step possessing a different magnitude. For example, the first current step was at 50 pA followed by 950, 1200, 1400, 1800, 2150, and 3200 pA. Eventually, the current flux reached 3650 pA and then a complete lipid bilayer failure occurred after 600 s of exposure. The normalized histogram shows multiple current peaks ranging from 26 pA to 3650 pA (0.26 nS to 36.5 nS) corresponding to the current steps recorded in Figure 2D. We observe similar behavior at lower (1.6 ppm) and higher (12 ppm) MWCNT concentrations as shown in Figure S2 D and E.

We believe that melittin and QDs disrupt the bilayer by similar mechanisms. They both show sporadic current spikes and both require several particles/molecules assembled to generate leakage. In contrast, MWCNTs show step-like currents that increase with time, suggesting that a different mechanism may be at work. We hypothesize that MWCNTs insert and traverse the lipid bilayer membrane, forming transmembrane channels that transport ions through the tube's core. The current steps increase as individual nanotubes span the bilayer, creating additional channels for ion transport.

Our hypothesis is supported by previous experimental and computational studies which have shown than CNTs can insert into or passively diffuse (i.e., endocytosis independent) across cell membranes.[26,24,20] These molecular dynamic simulations show that the insertion of CNTs into a biomembrane can occur in a spontaneous fashion. The CNT- lipid mechanism involves a two-step process, first the tubular particle adheres onto the membrane surface, and then reorients to adopt a transmembrane configuration. In a similar fashion, ions in an electrolyte have been shown to electromigrate through cores of CNT,[27,50,51] suggesting that our observed current flux may be made up of ions electromigrating through the core of CNTs that are inserted and span the suspended lipid bilayer. Lee et al. and Choi et al. measured ion transport through cores of CNT embedded within resins, which strongly supports our hypothesis.[52,53] They showed that current flux through the cores occurred with quantized current steps with stark similarity to our measurements shown in Figure 2D and Figure S2D and E. A definitive investigation of the mechanism in causing the bilayer current flux is ongoing work in our lab.

3.3 Quantification of Lipid Bilayer-ENPs Interactions

Our results suggest that different particles can induce significantly different current signatures (e.g., time to create a disturbance, current level, current burst length, etc.) which presents a challenge to quantitatively compare their interaction with the bilayer. Because the leakage caused by the ENP is a dynamic phenomenon, there are not obvious single-valued quantitative measures that can be used to assess the relative potential for ENP to disrupt a bilayer. Historically, current-time traces and histograms have been used to quantify electrophysiology measurements, yet these measures do not lend themselves well to comparison with varying particle properties or concentration. Here, we provide single-value, quantitative measures that can be potentially used to compare ENP against each other and other toxicity assays.

In this paper, we present the average conductance and the fraction event interaction (FEI) measure. The average conductance represents the average magnitude of all the lipid bilayer-nanoparticle interaction events integrated over a current-time trace plot, excluding the background noise events at I<10 pA, which corresponds to ~2 standards deviation from the mean current background noise. The FEI describes the fraction of time the bilayer is disrupted, defined as,

$$FEI = \sum_{j=j_{noise}}^{\infty} \frac{N_f}{\sum_j N_j} \quad 2$$

where j_{noise} is the bin associated with the background noise current at I=10 pA. This is equal to the area under the normalized histograms (e.g. Figure 2) excluding the area under the curves due to background nose, I=0–10 pA. The FEI is a measure of the fraction of time (0—1) that the particles disrupt the bilayer significantly from the background levels. A larger FEI for a particular particle indicates that the lipid membrane spends more time interacting over the recorded experiment duration. The average conductance and FEI values reported are averages of triplicate experiments at a fixed ENP mass concentration.

Figure 3 compares the fractional event interaction (FEI) of MWCNTs, QDs and melittin at several mass concentrations. The FEI increases with ENP number density (number of particles/per volume). Number density should directly correlate with the particle-membrane collision frequency, which should result in greater nanoparticle adsorption and subsequent leakage. Figure 4 shows the average conductance across the bilayer. The MWCNTs induced the largest average conductance ranging from 0.5 to 3.3 nS for mass concentrations of 1.6 to 12 ppm, respectively. QDs exhibited the lowest average conductance, which ranged from 0.20 to 0.45 nS for mass concentration of 6 to 60 ppm. We calculated the number density of the particles at 12 ppm as 2.5E15, 2E10, and 1.3E12 ml^{-1} for the melittin, MWCNT, and QDs, respectively. These results show that MWCNT exhibit stronger interactions with the bilayer with less than two orders of magnitude number density, consistent with the argument that the tube's interaction with the bilayer are distinct from the spherical particles and melittin.

Collectively, the average conductance and FEI measures show that the membrane disruption increases with mass concentration. The dose dependency can be attributed to a larger number of particles present, which results in a greater probability of particle contact with the lipid membrane. Although the average conductance and FEI combined allow a quantitative analysis that captures the average interaction behavior of nanoparticle and lipid bilayers, it does not reflect the specific interaction patterns (i.e., sporadic spikes versus stepwise current increase) and the eventual breakdown of lipid bilayer, which varies from particle to particle and can only be observed in the current-time traces. Thus, for a comprehensive and unbiased assessment of lipid bilayer-nanoparticle interactions, an analysis including the three pieces of information may be necessary.

4. SUMMARY

In this paper we report a direct measurement of ion migration across lipid bilayers induced by CNTs. Our results suggest that the distinctive current flux behavior for MWCNTs may be attributed to ions electromigrating through the core of CNTs that are inserted and span into the suspended lipid bilayer. Electrophysiological measurements enabled monitoring of ENP-lipid bilayer interaction dynamics in real time with millisecond temporal sensitivity. The diverse set of current traces suggests that the mode of bilayer disruption is dependent on the shape and concentration of particles. Furthermore, we presented a quantitative analysis (e.g., FEI and average conductance) of the interaction of ENPs-lipid membranes that captures the ion migration effect induced by particle shape, size and concentration. Given that cellular membrane disruption is one of the potential mechanisms leading to nano-toxicity, probing

the lipid bilayer disruption may provide insight into the nontoxicity mechanisms as well as a potential predictor of cytotoxicity studies for preliminarily screening of ENPs.

Supplementary Material

Refer to Web version on PubMed Central for supplementary material.

Acknowledgments

The United States Department of Energy (DE-FG02-08ER64613), National Science Foundation (CBET-0932885), NIH Grand Opportunities (RC2) program through NANO-GO NIEHS grant DE-FG02-08ER64613, Semiconductor Research Corporation (ERC-425.025), National Academies Ford Predoctoral Graduate Fellowship, National Science Foundation Graduate Fellowship, and More Graduate Education at Mountain State Alliance at ASU provided financial support. Also, the authors want to thank Prof. Somenath Mitra at the Department of Chemistry and Environmental Science at the New Jersey Institute of Technology for providing the MWCNTs, part of the NIEHS NANO-GO consortium, Jeffrey L. Moran for the valuable discussions, and William Walker for preparing BLM graphic.

References

1. Wiesner MR, Lowry GV, Alvarez P, Dionysiou D, Biswas P. Assessing the Risks of Manufactured Nanomaterials. Environmental Science & Technology. 2006 Jul 1; 40(14):4336–45. [PubMed: 16903268]
2. Nel A. Toxic Potential of Materials at the Nanolevel. Science. 2006 Feb; 311(5761):622–7. [PubMed: 16456071]
3. An inventory of nanotechnology-based consumer products currently on the market of the Project of Emerging Nanotechnology [Internet]. Project on Emerging Nanotechnologies. 2011. [cited 2011 Jul 7]. Available from: http://www.nanotechproject.org/inventories/consumer/analysis_draft/
4. Nel AE, Mädler L, Velegol D, Xia T, Hoek EMV, Somasundaran P, et al. Understanding biophysicochemical interactions at the nano–bio interface. Nat Mater. 2009 Jun; 8(7):543–57. [PubMed: 19525947]
5. Yan, Y; Such, GK; Johnston, APR; Best, JP; Caruso, F. Engineering Particles for Therapeutic Delivery: Prospects and Challenges. ACS Nano [Internet]. 2012. Available from:
6. Junhua, Yu; SandeepPatel, A; RobertDickson, M, 4. In Vitro and Intracellular Production of Peptide-Encapsulated Fluorescent Silver NanoclustersThe authors gratefully acknowledge financial support from NSF BES-0323453, Invitrogen Corp., NIH R01M68732, and NIH P20072021, and thank Prof. D. 4;F. Doyle for use of his cell-culture facility, and Prof. Y.-L. Tzeng for the gift of the peptides. Angewandte Chemie International Edition. 2007 Mar 12; 46(12):2028–30. [PubMed: 17285671]
7. Kostarelos K, Lacerda L, Pastorin G, Wu W, Sebastien Wieckowski, Luangsivilay J, et al. Cellular uptake of functionalized carbon nanotubes is independent of functional group and cell type. Nat Nano. 2007 Feb; 2(2):108–13.
8. Negoda A, Ying L, Hou W-C, Corredor C, Moghadam BY, Musolff C, et al. Engineered Nanomaterial Interactions with Bilayer Lipid Membranes: Screening Platforms to Assess Nanoparticle Toxicity. International Journal of Biomedical Nanoscience and Nanotechnology. 2012
9. Leroueil PR, Berry SA, Duthie K, Han G, Rotello VM, McNerny DQ, et al. Wide Varieties of Cationic Nanoparticles Induce Defects in Supported Lipid Bilayers. Nano Letters. 2008 Feb 1; 8(2): 420–4. [PubMed: 18217783]
10. Goodman CM, McCusker CD, Yilmaz T, Rotello VM. Toxicity of Gold Nanoparticles Functionalized with Cationic and Anionic Side Chains. Bioconjugate Chem. 2004; 15(4):897–900.
11. Moghadam, BY; Hou, W-C; Corredor, C; Westerhoff, P; Posner, JD. Role of Nanoparticle Surface Functionality in the Disruption of Model Cell Membranes. Langmuir [Internet]. 2012. Aug 24, [cited 2012 Oct 14]; Available from:
12. Hou W-C, Moghadam BY, Westerhoff P, Posner JD. Distribution of Fullerene Nanomaterials between Water and Model Biological Membranes. Langmuir. 2011 Sep 27; 27(19):11899–905. [PubMed: 21854052]

13. Hristovski KD, Westerhoff PK, Posner JD. Octanol-water distribution of engineered nanomaterials. J Environ Sci Health Part A-Toxic/Hazard Subst Environ Eng. 2011; 46(6):636–47.
14. Hou, W-C; Moghadam, BY; Corredor, C; Westerhoff, P; Posner, JD. Distribution of Functionalized Gold Nanoparticles between Water and Lipid Bilayers as Model Cell Membranes. Environ Sci Technol [Internet]. 2012. Available from:
15. Innovative Research and Products, Inc; 2011. Feb, Production and applications of carbon nanotubes, carbon nanofibers, fullerenes, graphene, and nanodiamonds: A global technology survey and market analysis [Internet]; 531Report No.: et-113. Available from: http://www.innoresearch.net/report_summary.aspx?id=77&pg=531&rcd=et-113&pd=2/1/2011
16. Lam C-W, James JT, McCluskey R, Arepalli S, Hunter RL. A review of carbon nanotube toxicity and assessment of potential occupational and environmental health risks. Crit Rev Toxicol. 2006 Mar; 36(3):189–217. [PubMed: 16686422]
17. Lewinski N, Colvin V, Drezek R. Cytotoxicity of Nanoparticles. Small. 2008 Jan 18; 4(1):26–49. [PubMed: 18165959]
18. Shvedova A, Castranova V, Kisin E, Schwegler-Berry D, Murray A, Gandelsman V, et al. Exposure to Carbon Nanotube Material: Assessment of Nanotube Cytotoxicity using Human Keratinocyte Cells. Journal of Toxicology and Environmental Health, Part A. 2003; 66(20):1909–26. [PubMed: 14514433]
19. Lamprecht C, et al. AFM imaging of functionalized carbon nanotubes on biological membranes. Nanotechnology. 2009; 20(43):434001. [PubMed: 19801758]
20. Porter AE, Gass M, Muller K, Skepper JN, Midgley PA, Welland M. Direct imaging of single-walled carbon nanotubes in cells. Nature Nanotech. 2007 Oct; 2(11):713–7.
21. De Paoli Lacerda SH, Semberova J, Holada K, Simakova O, Hudson SD, Simak J. Carbon Nanotubes Activate Store-Operated Calcium Entry (SOCE) in Human Blood Platelets. ACS nano. 2011
22. Semberova J, De Paoli Lacerda SH, Simakova O, Holada K, Gelderman MP, Simak J. Carbon Nanotubes Activate Blood Platelets by Inducing Extracellular Ca2+ Influx Sensitive to Calcium Entry Inhibitors. Nano Lett. 2009 Sep 9; 9(9):3312–7. [PubMed: 19736974]
23. Kang S, Mauter MS, Elimelech M. Physicochemical Determinants of Multiwalled Carbon Nanotube Bacterial Cytotoxicity. Environ Sci Technol. 2008; 42(19):7528–34. [PubMed: 18939597]
24. Shi X, von dem Bussche A, Hurt RH, Kane AB, Gao H. Cell entry of one-dimensional nanomaterials occurs by tip recognition and rotation. Nature Nanotechnology. 2011; 6(11):714–9.
25. Monticelli L, Salonen E, Ke PC, Vattulainen I. Effects of carbon nanoparticles on lipid membranes: a molecular simulation perspective. Soft Matter. 2009; 5(22):4433.
26. Lopez CF, Nielsen SO, Moore PB, Klein ML. Understanding nature's design for a nanosyringe. Proceedings of the National Academy of Sciences of the United States of America. 2004 Mar 30; 101(13):4431–4434. [PubMed: 15070735]
27. Liu B, Li X, Li B, Xu B, Zhao Y. Carbon Nanotube Based Artificial Water Channel Protein: Membrane Perturbation and Water Transportation. Nano Lett. 2009 Apr 8; 9(4):1386–94. [PubMed: 19245237]
28. Hummer G, Rasaiah JC, Noworyta JP. Water conduction through the hydrophobic channel of a carbon nanotube. Nature. 2001 Nov 8; 414(6860):188–90. [PubMed: 11700553]
29. Coronado R. Recent advances in planar phospholipid bilayer techniques for monitoring ion channels. Annual review of biophysics and biophysical chemistry. 1986; 15(1):259–77.
30. Goryll M, Wilk S, Laws GM, Thornton T, Goodnick S, Saraniti M, et al. Silicon-based ion channel sensor. Superlattices and Microstructures. 2003; 34(3):451–7.
31. Criado M, Keller BU. A membrane fusion strategy for single-channel recordings of membranes usually non-accessible to patch-clamp pipette electrodes. FEBS letters. 1987; 224(1):172–6. [PubMed: 2445602]
32. Agarwal A, Zudans I, Orwar O, Weber SG. Simultaneous Maximization of Cell Permeabilization and Viability in Single-Cell Electroporation Using an Electrolyte-Filled Capillary. Anal Chem. 2007 Jan; 79(1):161–7. [PubMed: 17194134]

33. Chen J, Hessler JA, Putchakayala K, Panama BK, Khan DP, Hong S, et al. Cationic Nanoparticles Induce Nanoscale Disruption in Living Cell Plasma Membranes. J Phys Chem B. 2009 Aug; 113(32):11179–85. [PubMed: 19606833]
34. Ramachandran S, Kumar GL, Blick RH, Van der Weide DW. Current bursts in lipid bilayers initiated by colloidal quantum dots. Applied Physics Letters. 2005 Feb 21.86(8):083901.
35. Klein SA, Wilk SJ, Thornton TJ, Posner JD. Formation of nanopores in suspended lipid bilayers using quantum dots. 2008; J Phys: Conf Ser. 109:012022.
36. De Planque MRR, Aghdaei S, Roose T, Morgan H. Electrophysiological Characterization of Membrane Disruption by Nanoparticles. ACS Nano. 2011 Sep 27; 5(5):3599–606. [PubMed: 21517083]
37. Wang X, Xia T, Ntim SA, Ji Z, George S, Meng H, et al. Quantitative Techniques for Assessing and Controlling the Dispersion and Biological Effects of Multiwalled Carbon Nanotubes in Mammalian Tissue Culture Cells. ACS Nano. 2010; 4(12):7241–52. [PubMed: 21067152]
38. Wang Y, Iqbal Z, Mitra S. Rapidly Functionalized, Water-Dispersed Carbon Nanotubes at High Concentration. J Am Chem Soc. 2005; 128(1):95–9.
39. Sessa G, Freer JH, Colacicco G, Weissmann G. Interaction of a Lytic Polypeptide, Melittin, with Lipid Membrane Systems. Journal of Biological Chemistry. 1969 Jul 10; 244(13):3575–3582. [PubMed: 5794226]
40. Pawlak M, Stankowski S, Schwarz G. Melittin induced voltage-dependent conductance in DOPC lipid bilayers. Biochimica et Biophysica Acta (BBA)-Biomembranes. 1991; 1062(1):94–102. [PubMed: 1998715]
41. Matsuzaki K, Yoneyama S, Miyajima K. Pore formation and translocation of melittin. Biophysical journal. 1997; 73(2):831–8. [PubMed: 9251799]
42. Edward JT. Molecular volumes and the Stokes-Einstein equation. J Chem Educ. 1970 Apr 1.47(4): 261.
43. Hunter, RJ. Zeta potential in colloid science: principles and applications. London; New York: Academic Press; 1981.
44. Bally, MB, Hope, MJ, Mayer, LD, Madden, TD, Cullis, PR. Liposomes as drug carriers: Recent trends and progress. Wiley; 1988. Novel procedures for generating and loading liposomal systems; 841–53.
45. Montal M, Mueller P. Formation of Bimolecular Membranes from Lipid Monolayers and a Study of their Electrical Properties. Proceedings of the National Academy of Sciences of the United States of America. 1972 Dec 1; 69(12):3561–6. [PubMed: 4509315]
46. Jain MK, Strickholm A, White FP, Cordes EH. Electronic Conduction across a Black Lipid Membrane. Nature. 1970; 227(5259):705–7. [PubMed: 5432068]
47. Tosteson MT, Tosteson DC. The sting. Melittin forms channels in lipid bilayers. Biophysical Journal. 1981; 36(1):109–16. [PubMed: 6269667]
48. Miller C, Moczydlowski E, Latorre R, Phillips M. Charybdotoxin, a protein inhibitor of single Ca2+-activated K+ channels from mammalian skeletal muscle. Nature. 1985 Jan 24; 313(6000): 316–8. [PubMed: 2578618]
49. Mecke A, Majoros IJ, Patri AK, Baker, Banaszak Holl MM, Orr BG. Lipid Bilayer Disruption by Polycationic Polymers: The Roles of Size and Chemical Functional Group. Langmuir. 2005; 21(23):10348–54. [PubMed: 16262291]
50. Joseph S, Mashl RJ, Jakobsson E, Aluru NR. Electrolytic Transport in Modified Carbon Nanotubes. Nano Lett. 2003; 3(10):1399–403.
51. Hilder TA, Gordon D, Chung SH. Synthetic Chloride-Selective Carbon Nanotubes Examined by Using Molecular and Stochastic Dynamics. Biophysical journal. 2010; 99(6):1734–42. [PubMed: 20858417]
52. Lee CY, Choi W, Han J-H, Strano MS. Coherence Resonance in a Single-Walled Carbon Nanotube Ion Channel. Science. 2010; 329(5997):1320–1324. [PubMed: 20829480]
53. Choi W, Lee CY, Ham M-H, Shimizu S, Strano MS. Dynamics of Simultaneous, Single Ion Transport through Two Single-Walled Carbon Nanotubes: Observation of a Three-State System. J Am Chem Soc. 2010; 133(2):203–5. [PubMed: 21166470]

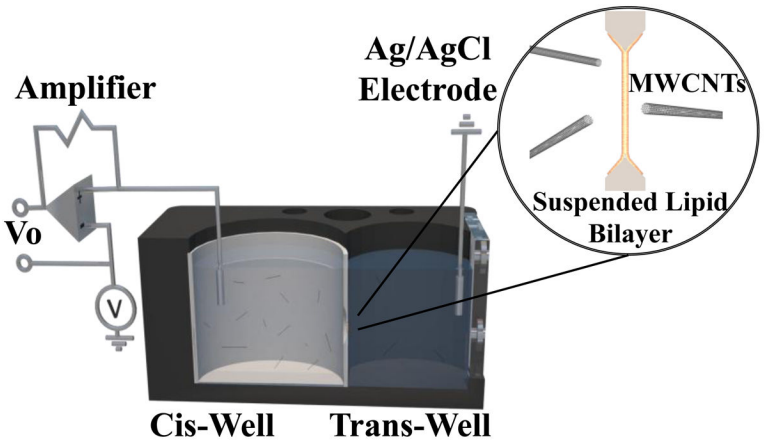

Figure 1.

Schematic of the experimental setup for electrophysiological measurements on pBLM. The ion migration across the bilayer is monitored using a low-noise amplifier and Ag/AgCl electrodes. A lipid bilayer is suspended across a 150-μm polystyrene aperture that separates the cis and trans well. ENPs (shown here as MWCNT) are added to the cis-well and disrupt the bilayer and results in an increase in the measured electrical current.

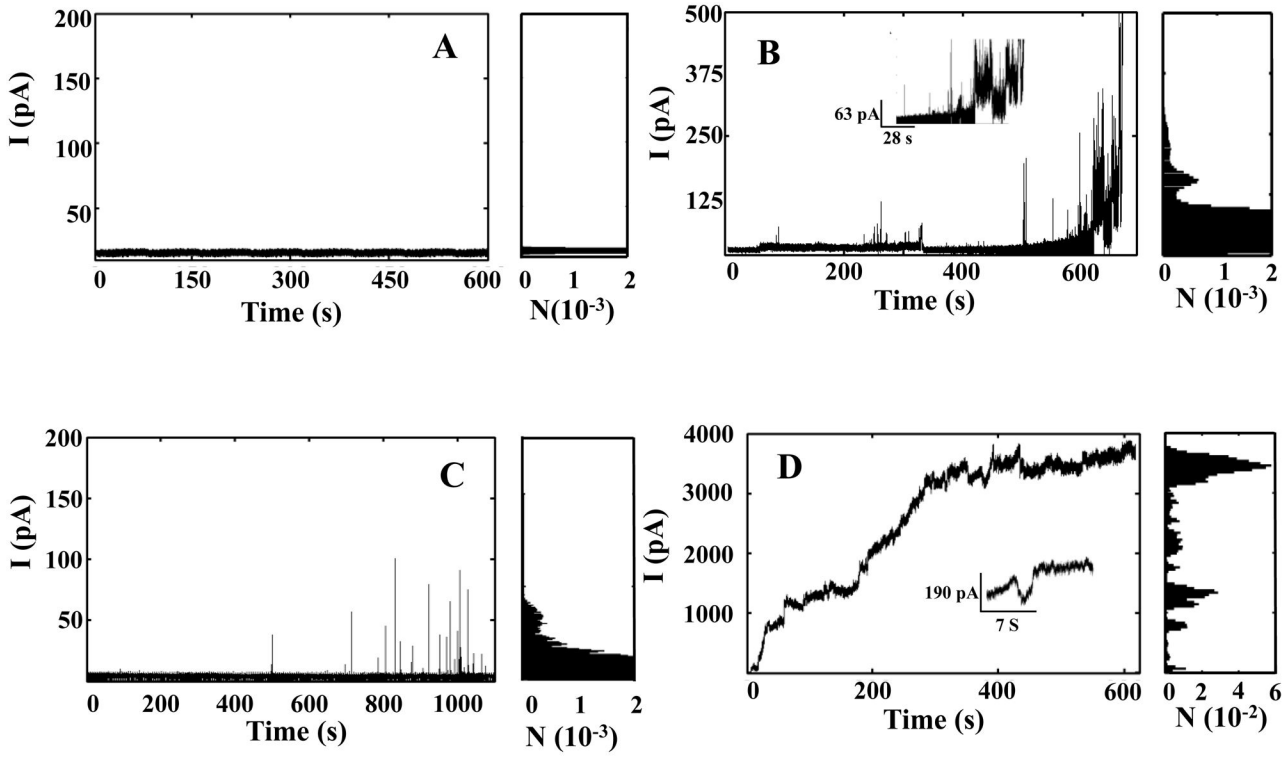

Figure 2.

Current-time traces of the and normalized current histograms with DOPC lipid bilayers at pH = 7.4 (20 mM HEPES and 20 mM KCl). (A) absence of nanoparticles; (B) melittin, a well-known pore forming peptide on lipid bilayers, at 6 ppm; (C) carboxyl quantum dots at 6 ppm; (D) functionalized multi-walled carbon nanotubes at 6 ppm.

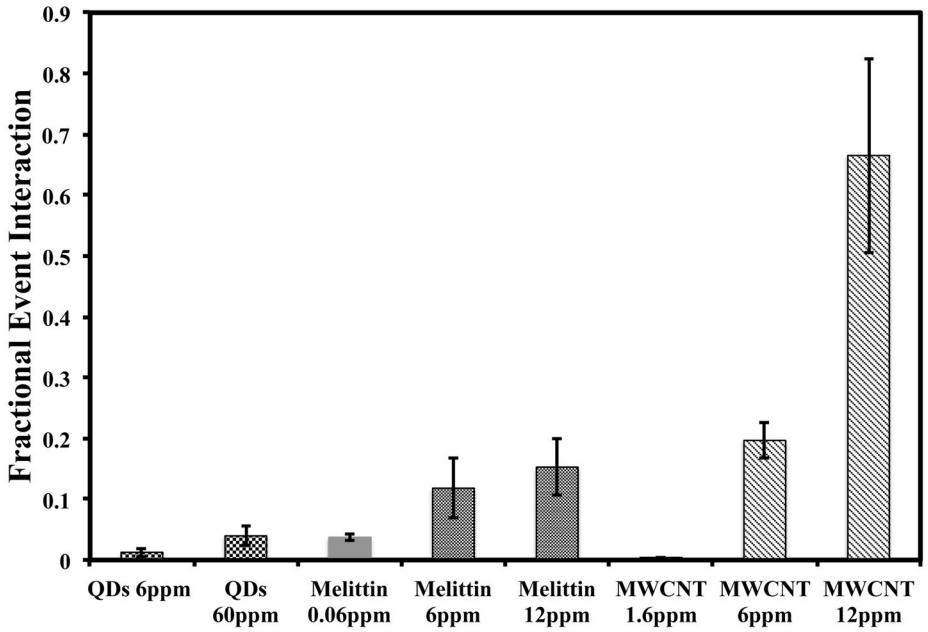

Figure 3.

Fractional event interaction of QD, MWCNT, and melittin with DOPC lipid bilayers at pH = 7.4 (20mM HEPES and 20mM KCl) at several nanoparticle concentrations. The fraction event interaction is a quantitative measure of the fraction of time that the nanomaterials disrupt the bilayer. The FEI increases with concentration and varies with particle composition and shape.

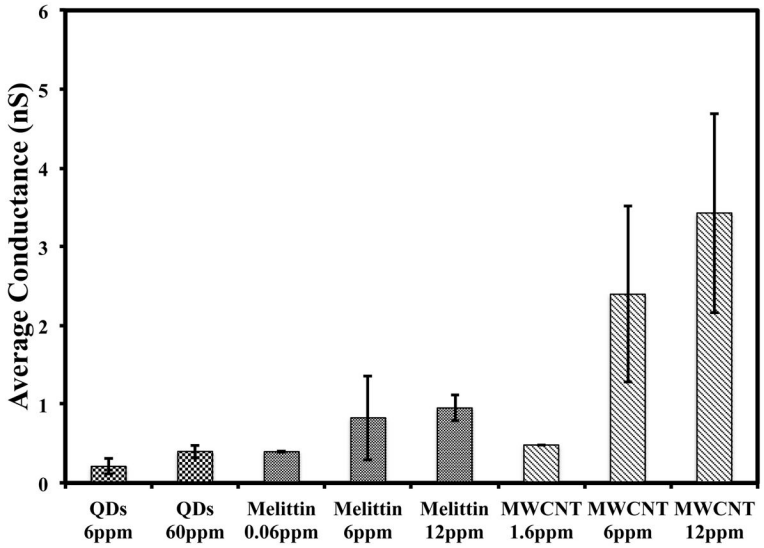

Figure 4.

Average conductance induced by QD, MWCNT, and melittin on DOPC lipid bilayers at pH = 7.4 (20mM HEPES and 20mM KCl) at several particle mass concentrations. The average conductance is calculated excluding the background signal.